Article:
Norcott, Philip, Burns, Michael J., Rayner, Peter J. et al. (2018) Using 2H Labelling to Improve the NMR detectability of a Series of Pyridines by SABRE. MAGNETIC RESONANCE IN CHEMISTRY. ISSN: 0749-1581

https://doi.org/10.1002/mrc.4703

Using ^{2}H Labelling to Improve the NMR Detectability of Pyridine and its Derivatives by SABRE

Philip Norcott, Michael J. Burns, Peter J. Rayner, Ryan E. Mewis and Simon B. Duckett*

Abstract

By introducing a range of ^{2}H labels into pyridine and the *para*-substituted agents methyl isonicotinate and isonicotinamide we significantly improve their NMR detectability in conjunction with the Signal Amplification by Reversible Exchange (SABRE) process. We describe how the rates of T_1 relaxation for the remaining ^{1}H nuclei are increased and show how this leads to a concomitant increase in the level of ^{1}H and ^{13}C hyperpolarization that can ultimately be detected.

Introduction

Hyperpolarization techniques overcome the inherent insensitivity of Nuclear Magnetic Resonance (NMR) and Magnetic Resonance Imaging (MRI) by manipulating the spin distribution across Zeeman-split energy levels away from equilibrium where a typical population difference used to produce a Magnetic Resonance (MR) signal can be less than 1 in 100 000. The employment of hyperpolarized states can therefore result in very substantial MR signal gains. This process can be achieved through a number of methods, the most common of which are Dynamic Nuclear Polarization (DNP)[1-3] and *Para*Hydrogen Induced Polarization (PHIP).[4-6] Signal Amplification By Reversible Exchange (SABRE)[7] has recently emerged as a powerful alternative that can rapidly and repeatedly hyperpolarize a substrate through the interaction of *para*hydrogen with an iridium catalyst. In SABRE, *para*hydrogen adds to a precatalyst, such as [IrCl(COD)(IMes)] (**1**, where IMes = 1,3-bis(2,4,6-trimethylphenyl)imidazol-2-ylidene and COD = *cis,cis*-cycloocta-1,5-diene), in the presence of a coordinating substrate (sub) to form an iridium hydride complex such as $[Ir(H)_2(IMes)(sub)_3]Cl$ (**2**)[8-9] (see Scheme 1). Polarization from the *para*hydrogen derived hydride ligands is then transferred into the bound substrate through the *J*-coupling network that exists in this complex.[10] Throughout the process, *para*hydrogen and the substrate which are located in the bulk solution are in reversible exchange with the corresponding ligands that are bound to the iridium complex. This results in a build-up of hyperpolarized substrate in bulk solution and hence the signal gain grows with *para*hydrogen exposure time, although a limit is reached because relaxation acts to destroy the hyperpolarization that has been created through SABRE.[11] As the rates of ligand exchange are relatively fast, substantial hyperpolarization levels can be produced in just a few seconds. SABRE has been demonstrated for a wide range of substrates which include pyridine and its derivatives,[9, 12-16] pyrazines,[16-17] imidazoles,[18-19] pyrazoles,[20-21] pyridazines,[22-24] pyrimidines,[25] amino acids,[26] diazirines,[27] and acetonitrile.[28] It hyperpolarizes not only their ^{1}H nuclei but the wide array of heteronuclei they contain.[19, 24-25, 29-30]

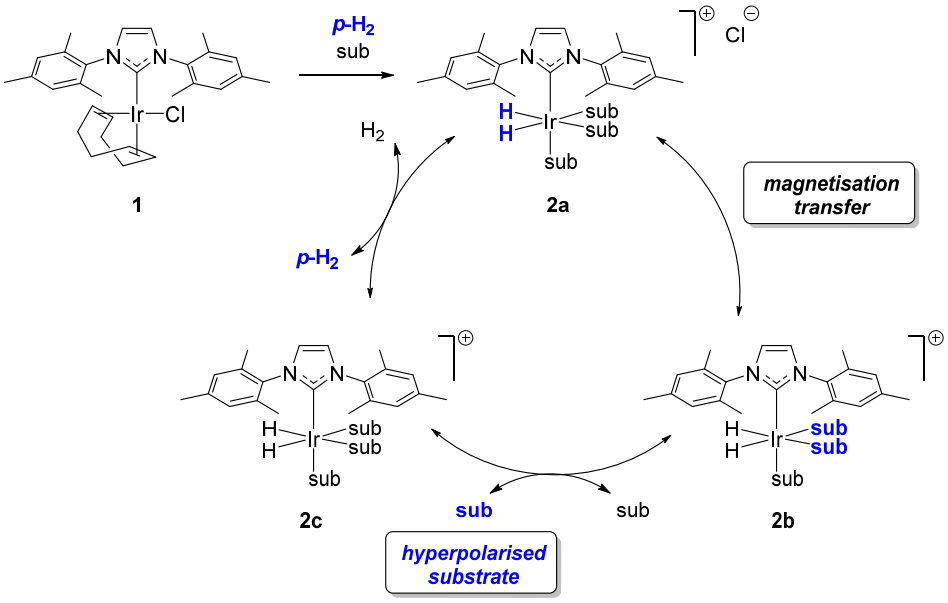

Scheme 1 Schematic representation of the Signal Amplification by Reversible Exchange (SABRE) process wherein the substrate (sub) achieves hyperpolarization through interactions within the metal complex **2a**.

It has recently been shown that the selective, partial ^{2}H-labelling of substrates such as pyridine,[13, 31] nicotinamide and methyl nicotinate greatly extends the T_1 relaxation times of the remaining ^{1}H-nuclei through inhibition of scalar relaxation processes.[14, 32-33] In addition, through ^{2}H-labelling of the IMes ligand of the iridium catalyst, the relaxation times of the bound substrate increase which further results in a dramatic improvement in the ^{1}H hyperpolarization levels that can be achieved through SABRE. In fact, they exceed 50% polarization when 5 bar of parahydrogen is used in conjunction with a co-ligand.[14] In this current work, we seek to report further developments that employ this ^{2}H-labelling strategy by applying it to the related compounds pyridine, methyl isonicotinate and isonicotinamide. We seek to ascertain its effect on the efficacy of the resulting ^{1}H and ^{13}C hyperpolarization levels that can be achieved through SABRE.

Results and Discussion

Pyridine (**3**) was one of the first compounds to be hyperpolarized by the SABRE method.[7, 12, 15] Because of its relatively simple structure, we recognised that there was an opportunity to investigate the effect of selective ^{2}H labelling on the level of hyperpolarization. A selection of selectively deuterated pyridines shown in Figure 1 were therefore synthesised.[34-35] This approach gave us access to three isotopologues of pyridine, **3a**, **3b** and **3c**, in which ^{1}H-nuclei are retained at the *ortho*, *meta* and *para* positions of the ring respectively.

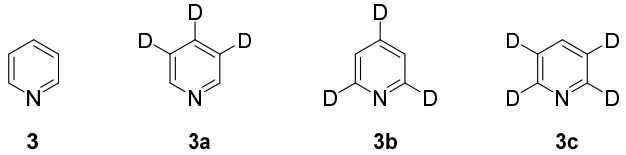

Figure 1 ^{2}H-labelled pyridine isotopologues used in this study.

When *protio*-pyridine **3** (20 mM, 4 eq.) is mixed with [IrCl(COD)IMes] (5 mM) and *para*hydrogen in ethanol-d_6 and shaken at 65 gauss for 10 seconds followed by immediate transport into the spectrometer for detection, the signal for H_a in Fig. 2 appears with an intensity that is *ca.* 2400 larger than that observed under Boltzmann conditions in the corresponding thermally equilibrated control measurement. In contrast, the corresponding signals for H_b and H_c are 1120 and 1258 times larger than those of the corresponding reference signals (at 9.4 T). Fig. 2 (*left*) illustrates a typical measurement. The new signal intensity reflects the detection of 3.9% H_a polarization, created after just 10 seconds of exposure to 3 bar of *para*hydrogen. Furthermore, we note that if 20 seconds were needed to repeat the control measurement which uses thermally equilibrated polarization levels, it would take 1333 days of data averaging to reproduce the hyperpolarized signal intensity. It is for this reason that hyperpolarization reflects a method that could transform clinical diagnosis as it may facilitate the facile detection of markers that probe underlying physiology.[36]

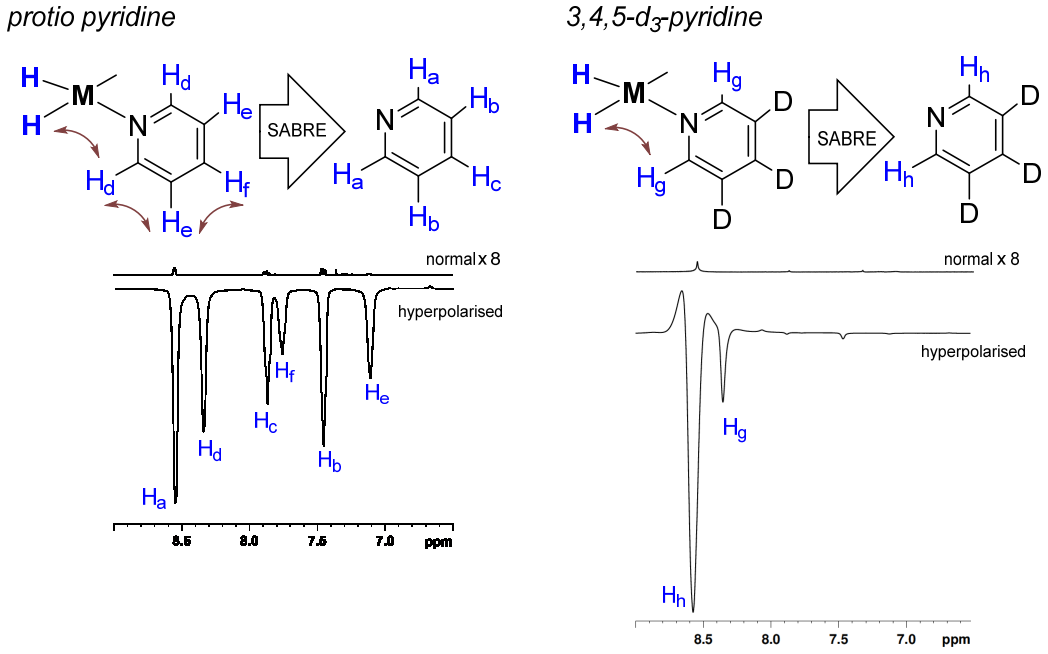

Fig. 2 *Left*: Two single scan ^{1}H NMR spectra which illustrate pyridine (**3**) signals (attributed according to inset scheme) that result after SABRE (hyperpolarised) and when the polarization level matches that for thermodynamic equilibrium (normal). *Right*: Two similar single scan ^{1}H NMR spectra employing **3a**. The normal traces are shown with a ×8 vertical expansion relative to the hyperpolarised trace.

When the agent 3,4,5-d_3-pyridine (**3a**) was employed under identical conditions to those described for **3**, the signal enhancement seen for the remaining *ortho* protons increases to 4166 (6.7% polarization), shown in Table 1. However, upon moving to 2,4,6-d_3-pyridine (**3b**), the remaining *meta* protons exhibit a smaller gain associated with an enhancement of just 541 (0.9% polarization). Finally, 2,3,5,6-d_4-pyridine (**3c**) results in very little signal gain with its remaining proton showing a 163-fold enhancement (0.51% polarization). These values are the average of three distinct measurements and are hence reproducible.

The lower polarization levels seen for **3b** and **3c** can be rationalized as the result of the fact that their protons are magnetically isolated from those of the hydride ligands in the iridium catalyst. Hence,

smaller *J*-couplings are involved in the polarisation transfer step and less effective SABRE transfer results.[37] By comparison, **3a** features two *ortho* ^{1}H-nuclei which couple more strongly to the hydride ligands in the SABRE-catalyst and they are therefore able to more readily receive magnetization. An analogous trend was found when methanol-d_4 was used as the solvent and in this case a polarization level of 5.8% could be achieved with **3a**.

The reduction in hydride-substrate *J*-coupling is somewhat offset by relaxation changes. At 400 MHz, in degassed ethanol-d_6, *protio*-pyridine (**3**) was found to exhibit T_1 relaxation times of between 18.2 and 26.7 seconds (Table 1). Its isotopologue **3a**, however, has relaxation times for the two *ortho* protons of 72.4 seconds, while in **3b** the *meta* protons exhibit a 72.6 second value and in **3c** the *para* proton has a T_1 of 57.5 seconds. The values determined in the ^{2}H-labelled isotopologues therefore reflect a dramatic improvement on those of the unlabelled **3**. We note, however, that under the catalytic conditions used in SABRE, interactions with the iridium catalyst act to reduce the observed T_1 values. This is because the free and bound forms are in equilibrium and the observed value therefore reflects a weighted average of the two. For unlabelled pyridine, the new values lie between 3.2 and 5.3 seconds, while for **3a**, **3b** and **3c** they are 4.2, 13.8 and 25.0 seconds respectively. As percentages, the reductions caused by the presence of the catalyst in solution are therefore 94%, 81% and 56% respectively. This serves to demonstrate that the effect is most strongly manifest in the *ortho* protons which exhibit the strongest spin-spin coupling to the hydride ligands when bound to the iridium. While **3b** exhibits a better T_1 value for the *meta* position, it fails to receive strong magnetisation through SABRE, a feature that is strongly demonstrated for the *para* proton of **3c**. Again, analogous relaxation and polarization trends were observed in methanol-d_4 solution. However, relaxation times for **3b** and **3c** were significantly extended in methanol-d_4, compared to ethanol-d_6.

Hence we can conclude it is desirable to locate a proton next to the catalyst binding site, where J_{HH} is maximised, for optimal SABRE activity but we tension this need with the fact that such an arrangement will also reduce the effective lifetime of the polarization under catalytic conditions. Clearly, the interplay between the T_1 of the proton site and the efficacy of polarisation transfer must therefore be carefully considered when designing an optimised agent.

Table 1 T_1 relaxation times and polarization levels achieved for pyridines **3** through SABRE in the specified solvent. *Conditions:* 20 mM substrate, 5 mM [IrCl(COD)IMes], activated with 3 bar *p*-H_2. *o* = *ortho*, *m* = *meta*, *p* = *para*.

Substrate		Methanol-d_4			Ethanol-d_6		
		Site $T_{1(\text{no cat.})}$ / s	Site $T_{1(\text{with cat.})}$ /s	Polarization Level (%)	Site $T_{1(\text{no cat.})}$ / s	Site $T_{1(\text{with cat.})}$ /s	Polarization Level (%)
	**3**	*o* – 28.1 *m* – 26.2 *p* – 33.8	*o* – 1.5 *m* – 5.2 *p* – 5.5	*o* – 4.3 ± 0.3 *m* – 3.4 ± 0.1 *p* – 5.4 ± 0.1	*o* – 20.7 *m* – 18.2 *p* – 26.7	*o* – 3.2 *m* – 4.7 *p* – 5.3	*o* – 3.9 ± 0.2 *m* – 1.8 ± 0.1 *p* – 4.0 ± 0.1
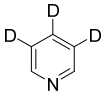	**3a**	*o* – 51.2	*o* – 5.2	*o* – 5.8 ± 0.4	*o* – 72.4	*o* – 4.2	*o* – 6.9 ± 0.4
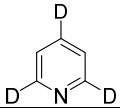	**3b**	*m* – 113.2	*m* – 46.7	*m* – 0.6 ± 0.1	*m* – 72.6	*m* – 13.8	*m* – 1.0 ± 0.1

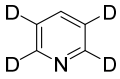 **3c**	*p* – 84.7	*p* – 67.0	*p*–0.54 ± 0.12	*p* – 57.5	*p* – 25.0	*p* – 0.51 ± 0.07

A series of hyperpolarized ^{13}C measurements were then conducted using 3,4,5-d_3-pyridine (**3a**) in the presence of **1** for a 4:1 loading after SABRE at approximately 0.5 G. The resulting fully coupled single-scan ^{13}C hyperpolarized NMR spectrum is shown in Fig. 3 alongside its thermally equilibrated ^{13}C counterpart which is a 2048 scan average. A significant increase in the ^{13}C resonances' signal-to-noise ratios is clearly observed in the hyperpolarized spectrum. Furthermore, the *ortho* peak (148 ppm) is observed as an antiphase doublet of doublets, whereas the *meta* (124 ppm) and *para* (137 ppm) peaks are split into antiphase triplets of doublets. This is consistent with the creation of I_zS_z terms, where the antiphase component is associated with the small, indirect J_{HC} coupling. The *meta* and *para* signals are associated with the detection of a ^{13}CD signal for the *meta* and *para* sites which accounts for the in-phase 1:1:1 splitting.

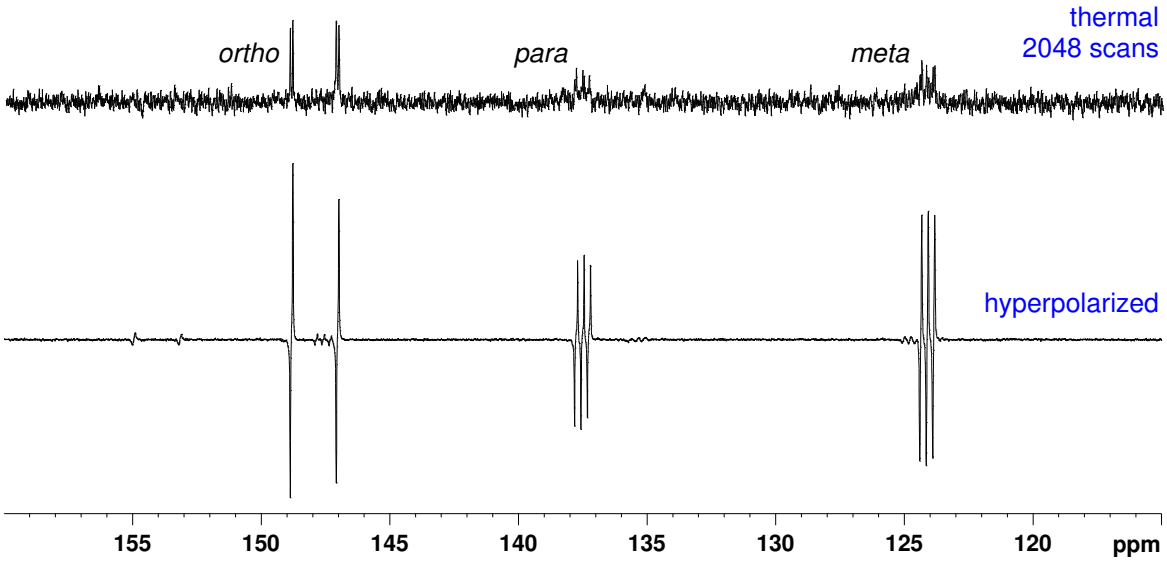

Fig. 3 *Top*: Thermal ^{13}C NMR spectrum of **3a** (100 mM) and SABRE catalyst (5 mM) in methanol-d_4 after 2048 scans. *Bottom*: Single-scan hyperpolarized ^{13}C NMR spectrum.

When a similar experiment was recorded with concurrent ^{1}H decoupling a much weaker signal was observed (Fig. 4). This confirms that the dominant terms that are created under SABRE at 60 G are indeed I_zS_z based rather than S_z. We expect that the levels of signal gain that are observed may be improved through the incorporation of a ^{15}N label, which has recently been shown to reduce ^{13}C polarization transfer losses due to quadrupolar relaxation.[38]

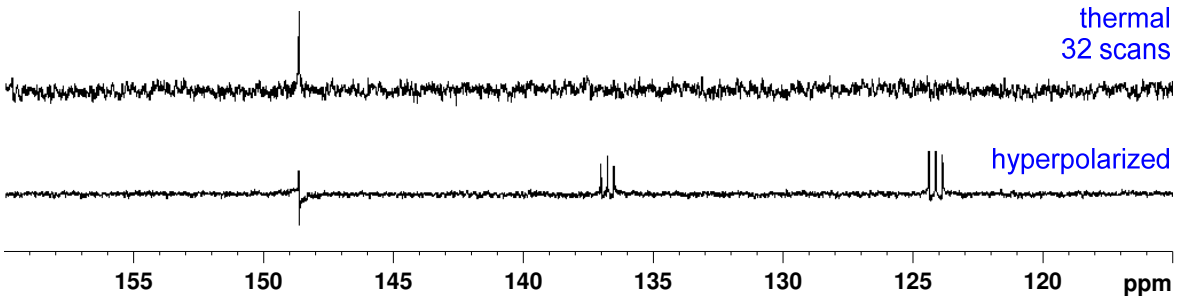

Fig. 4 *Top*: Thermal $^{13}C\{^1H\}$ NMR spectrum of **3a** (100 mM) and SABRE catalyst (5 mM) in methanol-d_4 over 32 scans. *Bottom*: Single-scan hyperpolarized $^{13}C\{^1H\}$ NMR spectrum.

Following these observations, we turned our attention to the *para*-substituted pyridine derivatives, methyl isonicotinate (**4**) and isonicotinamide (**5**). A range of doubly deuterated isotopologues of these compounds were synthesized according to Scheme 2, and the results of the related NMR studies are shown in Table 2. These substrates provide a range of ^1H spin systems, and we expected them to exhibit markedly different hyperpolarization characteristics. This reflects the fact that **4a** and **5a** possess pairs of *ortho* and *meta* ^1H nuclei that exhibit a mutual 3-bond coupling, in contrast, **4b** and **5b** contain two weakly coupled *ortho* and *meta* nuclei (5-bond coupling), while **4c, 5c, 4d** and **5d** contain pairs of equivalent *ortho* and *meta* nuclei respectively.

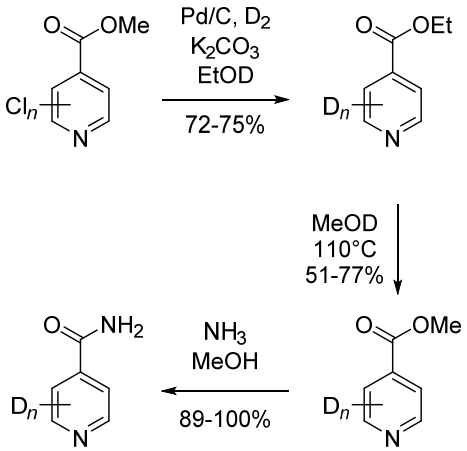

Scheme 2 Synthetic route to the doubly ^2H-labelled methyl isonicotinates **4** and isonicotinamides **5**.

For these ester and amide substrates, deuteration at the 2- and 3- positions (**4a** and **5a**) proved to result in limited changes in there relaxation times relative to their ^1H counterpart and somewhat similar polarization levels as a result of SABRE were observed (Table 2). These results indicate that relaxation within these molecules is driven by interactions between the adjacent ^1H nuclei. Analogues **b-d**, with more isolated ^1H spin systems, might therefore be predicted to have higher T_1 values. In support of this, we found that deuteration at the 2- and 5-positions (**4b** and **5b**) does indeed result in significantly improved relaxation times, and SABRE polarization levels. Now the T_1 values are over 60 seconds for methyl 2,5-d_2-isonicotinate **4b**, which compare to 14 seconds of

protio **4**. In the case of isonicotinamide **5b**, the SABRE polarization levels actually improve from the original 2.6% and 0.2% levels for the *ortho* and *meta* positions of **5** (in methanol-d_4) respectively to 12.4% and 12.3% respectively. In this case, the extension of the T_1 values determined for the *meta* proton in the presence of the SABRE catalyst greatly assists in increasing the observed polarization level of the proton at this position.

In general, compounds with only *ortho* ^{1}H-nuclei (**4c** and **5c**) gave slightly improved levels of polarization and T_1 values that compare to those of the parent, but still suffer from short relaxation times when determined in the presence of the SABRE catalyst. This is consistent with the results outlined earlier for **3a**. Compounds **4d** and **5d**, with only *meta* ^{1}H nuclei now give higher T_1 values, but as expected, the improvement in achieved polarization level is minimal, in accordance with the weaker *J*-coupling that connects them to hydride ligands in the catalyst.

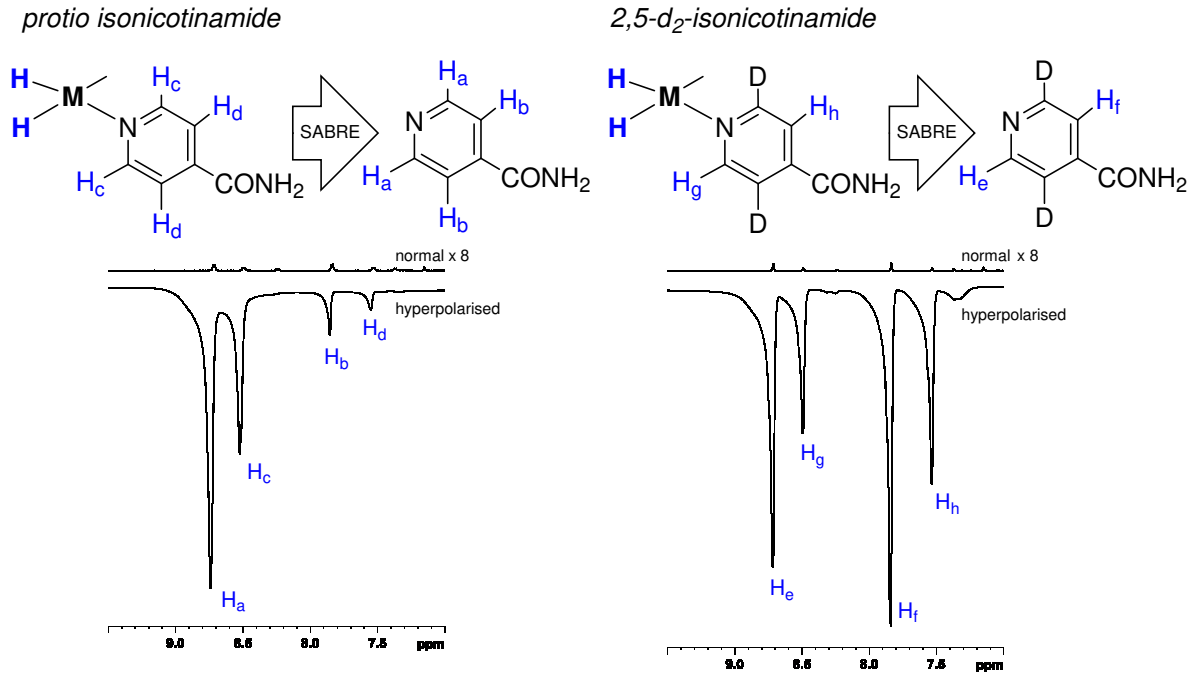

Fig. 5 *Left*: Single scan ^{1}H NMR spectra for hyperpolarized and fully relaxed isonicotinamide **5** at 400 MHz. *Right*: Corresponding single scan ^{1}H NMR spectra of **5b**. The normal traces are shown with a ×8 vertical expansion relative to the hyperpolarised traces.

Table 2 T_1 relaxation times (s) and polarization levels found for the methyl isonicotinates **4** and the isonicotinamides **5**. *Conditions:* 20 mM substrate, 5 mM [IrCl(COD)IMes], activated with 3 bar *p*-H_2. *o* = *ortho*, *m* = *meta*.

Substrate		**Methanol-d_4**		
		Site $T_{1(\text{no cat.})}$ / s	**Site $T_{1(\text{with cat.})}$ /s**	**Polarization Level (%)**
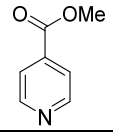	**4**	*o* – 14.2 *m* – 14.1	*o* – 1.9 *m* – 3.9	*o* – 4.8 ± 0.1 *m* – 1.0 ± 0.1

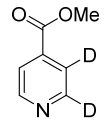	**4a**	*o* – 9.6 *m* – 9.6	*o* – 2.9 *m* – 5.8	*o* – 2.2 ± 0.1 *m* – 1.4 ± 0.1
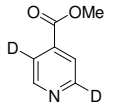	**4b**	*o* – 61.9 *m* – 61.2	*o* – 3.5 *m* – 21.4	*o* – 5.4 ± 0.4 *m* – 5.6 ± 0.3
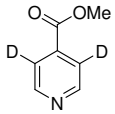	**4c**	*o* – 70.7	*o* – 4.1	*o* – 7.4 ± 0.3
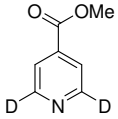	**4d**	*m* – 72.8	*m* – 16.1	*m* – 7.4 ± 0.4
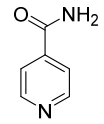	**5**	*o* – 8.2 *m* – 8.3	*o* – 1.7 *m* – 3.5	*o* – 2.6 ± 0.2 *m* – 0.2 ± 0.02
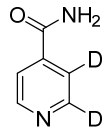	**5a**	*o* – 7.4 *m* – 8.3	*o* – 2.3 *m* – 4.1	*o* – 3.5 ± 0.3 *m* – 0.4 ± 0.1
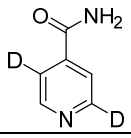	**5b**	*o* – 18.2 *m* – 42.7	*o* – 4.2 *m* – 16.0	*o* – 11.0 ± 0.5 *m* – 11.1 ± 0.5
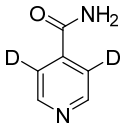	**5c**	*o* – 23.4	*o* – 2.9	o – 5.8 ± 0.7
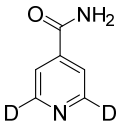	**5d**	*m* – 47.2	*m* – 8.3	*m* – 4.2 ± 0.1

These trends confirm our earlier conclusions that substrates containing a ^{1}H nucleus at the *ortho* position result in efficient polarization transfer and that ^{1}H nuclei which are isolated from each other, and the hydride ligands of the metal catalyst, lead to increased relaxation times under SABRE. These changes contribute cooperatively to produce a strong, long-lived hyperpolarised signal.

Related hyperpolarised ^{13}C NMR experiments on the labelled isonicotinamides (**5a**-**5d**) showed that superior signal enhancements could be achieved with these substrates (Fig. 6). With a 20-fold concentration of substrate to catalyst and polarization transfer at approximately 0.5 gauss, compound **5a** showed strong SABRE responses for the quaternary carbons, including those adjacent to the ^{2}H-labels. The remaining CH positions showed a much lower, but detectable signal enhancement, an effect which is predicted to be due to an increased rate of relaxation. Compound **5b** produced a similar outcome; the higher levels of ^{1}H polarization enabling increased magnetization transfer to be relayed into the most distant quaternary carbon. In the case of compound **5c**, a clear SABRE signal was observed for all carbons on the aromatic ring, notably

including that of the CH at the *ortho* position. The carbonyl carbon showed significantly smaller polarization, as only a weak $^{4}J_{CH}$ coupling to the ortho proton is possible from that site for transfer. Analogue **5d** gave very little ^{13}C polarization, with only the carbonyl position being visible. It should be noted that in all cases the dominant peaks appear in anti-phase due to the observation of I_zS_z derived states.

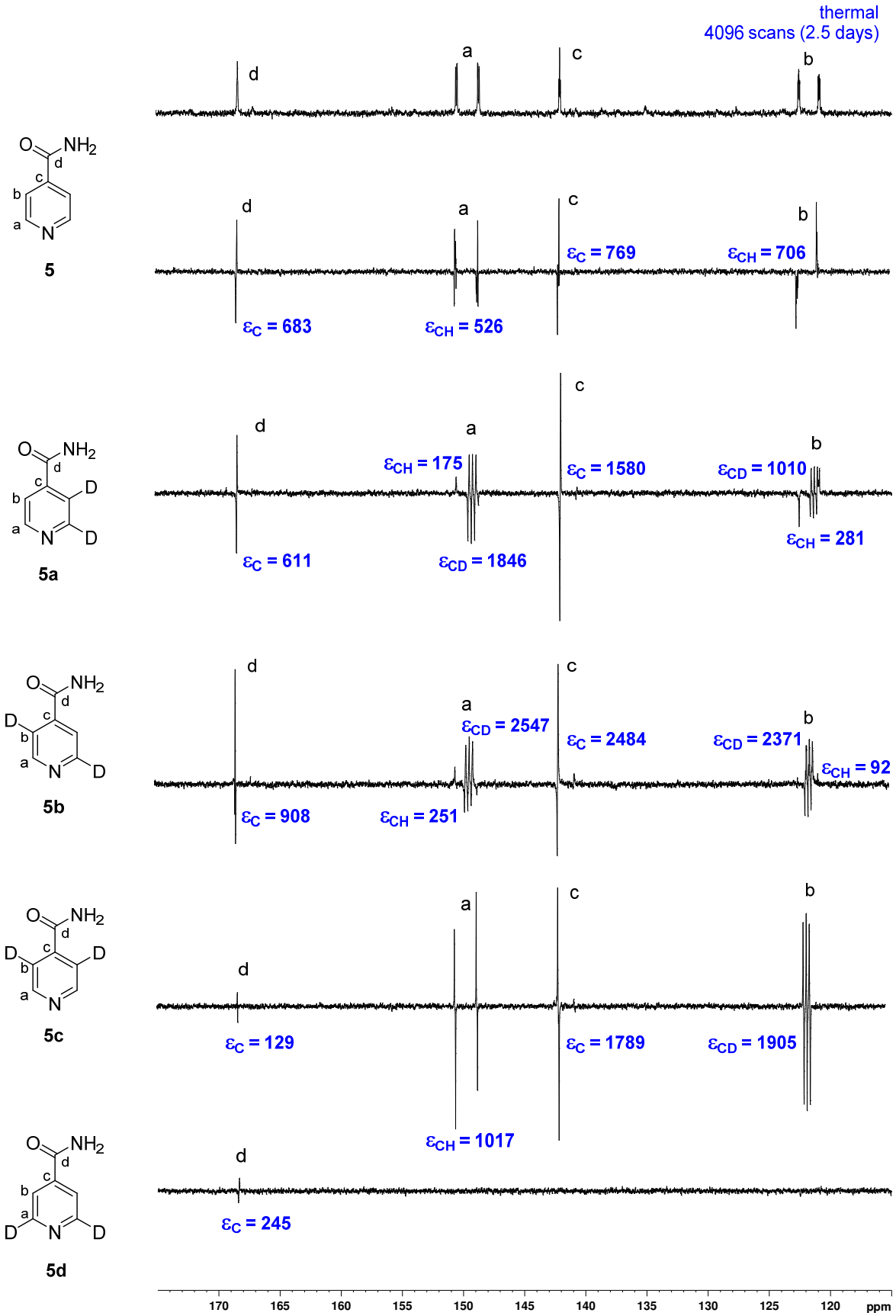

Fig. 6 Series of hyperpolarized single-scan ^{13}C NMR spectra of **5-5d** (100 mM) and [IrCl(COD)(IMes)] (5 mM) in methanol-d_4 under *p*-H_2 after transfer at 0.5 G. Thermally polarized reference ^{13}C NMR spectrum (top), acquired over 4096 scans. ε = enhancement factor, fold gain.

Conclusions

An investigation has been made into the effect of selectively incorporating ^{2}H labels into a number of pyridine-based substrates and the subsequent effect this change had on the observed hyperpolarization levels achieved through the SABRE process. We completed studies on three isotopologues of pyridine (**3**), four isotopologues of methyl isonicotinate (**4**) and four isotopologues of isonicotinamide (**5**). We find that harnessing hyperpolarization sites adjacent to the nitrogen centre of pyridine, which binds to the SABRE catalyst metal centre, is crucial for efficient polarization transfer through its stronger $^{4}J_{HH}$ coupling to the *para*hydrogen-derived metal hydride ligands. Furthermore, we confirm that the presence of spin-isolated hyperpolarization sites in these agents both increases signal lifetime through reduced relaxation, and allows the detection of strongly hyperpolarized ^{1}H responses. These changes also facilitate the detection of strong ^{13}C NMR signals, most notably for the corresponding quaternary and CD positions. These signals typically appear with anti-phase character due their origin in a heteronuclear longitudinal two spin order term (^{1}H-^{13}C) involving an indirect coupling. Agent **5b** produced the strongest carbonyl signal as a consequence of a $^{3}J_{HC}$ coupling, which must lead to limited internal peak cancelation due to its small value. In contrast the larger ^{13}C-$CONH_2$ response results with **5a**. The ^{13}CH signals of **5c** are also dramatically stronger than those of **5a**, **5b** and **5d** in accordance with a predicted long relaxation time. The spin isolation of the C-$^{13}CONH_2$ groups in **5c** and **5d** though acts to reduce its detectability, although the signal for C-$^{13}CONH_2$ is strongly visible in **5a** and **5b**. Hence we conclude that a ^{2}H labelling strategy can be used to not only control ^{1}H signal gains, but also those of ^{13}C. We expect that this strategy will enable improvement in polarization in molecules containing other heteronuclei, such as ^{15}N, and work is ongoing to achieve this goal. Additionally, a detailed investigation into the mechanism of polarization transfer in molecules containing ^{2}H nuclei would be of interest.

Acknowledgements

We thank the Wellcome Trust (092506 and 098335) for funding.

ORCID

Philip Norcott http://orcid.org/0000-0003-4082-2079

Michael J. Burns http://orcid.org/0000-0002-5569-1270

Peter J. Rayner http://orcid.org/0000-0002-6577-4117

Simon B. Duckett http://orcid.org/0000-0002-9788-6615

References

1. Ardenkjær-Larsen, J. H.; Fridlund, B.; Gram, A.; Hansson, G.; Hansson, L.; Lerche, M. H.; Servin, R.; Thaning, M.; Golman, K., Increase in signal-to-noise ratio of > 10,000 times in liquid-state NMR. *Proc. Natl. Acad. Sci. U.S.A.* **2003,** *100* (18), 10158-10163.
2. Keshari, K. R.; Wilson, D. M., Chemistry and biochemistry of 13C hyperpolarized magnetic resonance using dynamic nuclear polarization. *Chem. Soc. Rev.* **2014,** *43* (5), 1627-1659.

3. Ardenkjaer-Larsen, J. H., On the present and future of dissolution-DNP. *J. Magn. Reson.* **2016,** *264* (Supplement C), 3-12.
4. Bowers, C. R.; Weitekamp, D. P., Transformation of Symmetrization Order to Nuclear-Spin Magnetization by Chemical Reaction and Nuclear Magnetic Resonance. *Phys. Rev. Lett.* **1986,** *57* (21), 2645-2648.
5. Bowers, C. R.; Weitekamp, D. P., Parahydrogen and synthesis allow dramatically enhanced nuclear alignment. *J. Am. Chem. Soc.* **1987,** *109* (18), 5541-5542.
6. Golman, K.; Axelsson, O.; Jóhannesson, H.; Månsson, S.; Olofsson, C.; Petersson, J. S., Parahydrogen-induced polarization in imaging: Subsecond 13C angiography. *Magn. Reson. Med.* **2001,** *46* (1), 1-5.
7. Adams, R. W.; Aguilar, J. A.; Atkinson, K. D.; Cowley, M. J.; Elliott, P. I. P.; Duckett, S. B.; Green, G. G. R.; Khazal, I. G.; López-Serrano, J.; Williamson, D. C., Reversible Interactions with para-Hydrogen Enhance NMR Sensitivity by Polarization Transfer. *Science* **2009,** *323* (5922), 1708-1711.
8. Cowley, M. J.; Adams, R. W.; Atkinson, K. D.; Cockett, M. C. R.; Duckett, S. B.; Green, G. G. R.; Lohman, J. A. B.; Kerssebaum, R.; Kilgour, D.; Mewis, R. E., Iridium N-Heterocyclic Carbene Complexes as Efficient Catalysts for Magnetization Transfer from para-Hydrogen. *J. Am. Chem. Soc.* **2011,** *133* (16), 6134-6137.
9. Lloyd, L. S.; Asghar, A.; Burns, M. J.; Charlton, A.; Coombes, S.; Cowley, M. J.; Dear, G. J.; Duckett, S. B.; Genov, G. R.; Green, G. G. R.; Highton, L. A. R.; Hooper, A. J. J.; Khan, M.; Khazal, I. G.; Lewis, R. J.; Mewis, R. E.; Roberts, A. D.; Ruddlesden, A. J., Hyperpolarisation through reversible interactions with parahydrogen. *Catal. Sci. Technol.* **2014,** *4* (10), 3544-3554.
10. Adams, R. W.; Duckett, S. B.; Green, R. A.; Williamson, D. C.; Green, G. G. R., A theoretical basis for spontaneous polarization transfer in non-hydrogenative parahydrogen-induced polarization. *J. Chem. Phys.* **2009,** *131* (19), 194505.
11. Barskiy, D. A.; Pravdivtsev, A. N.; Ivanov, K. L.; Kovtunov, K. V.; Koptyug, I. V., A simple analytical model for signal amplification by reversible exchange (SABRE) process. *PCCP* **2016,** *18* (1), 89-93.
12. Atkinson, K. D.; Cowley, M. J.; Elliott, P. I. P.; Duckett, S. B.; Green, G. G. R.; López-Serrano, J.; Whitwood, A. C., Spontaneous Transfer of Parahydrogen Derived Spin Order to Pyridine at Low Magnetic Field. *J. Am. Chem. Soc.* **2009,** *131* (37), 13362-13368.
13. Hövener, J.-B.; Schwaderlapp, N.; Borowiak, R.; Lickert, T.; Duckett, S. B.; Mewis, R. E.; Adams, R. W.; Burns, M. J.; Highton, L. A. R.; Green, G. G. R.; Olaru, A.; Hennig, J.; von Elverfeldt, D., Toward Biocompatible Nuclear Hyperpolarization Using Signal Amplification by Reversible Exchange: Quantitative in Situ Spectroscopy and High-Field Imaging. *Anal. Chem.* **2014,** *86* (3), 1767-1774.
14. Rayner, P. J.; Burns, M. J.; Olaru, A. M.; Norcott, P.; Fekete, M.; Green, G. G. R.; Highton, L. A. R.; Mewis, R. E.; Duckett, S. B., Delivering strong 1H nuclear hyperpolarization levels and long magnetic lifetimes through signal amplification by reversible exchange. *Proc. Natl. Acad. Sci. U.S.A.* **2017,** *114* (16), E3188-E3194.
15. Atkinson, K. D.; Cowley, M. J.; Duckett, S. B.; Elliott, P. I. P.; Green, G. G. R.; López-Serrano, J.; Khazal, I. G.; Whitwood, A. C., Para-Hydrogen Induced Polarization without Incorporation of Para-Hydrogen into the Analyte. *Inorg. Chem.* **2009,** *48* (2), 663-670.
16. Zeng, H.; Xu, J.; Gillen, J.; McMahon, M. T.; Artemov, D.; Tyburn, J.-M.; Lohman, J. A. B.; Mewis, R. E.; Atkinson, K. D.; Green, G. G. R.; Duckett, S. B.; van Zijl, P. C. M., Optimization of SABRE for polarization of the tuberculosis drugs pyrazinamide and isoniazid. *J. Magn. Reson.* **2013,** *237*, 73-78.
17. Roy, S. S.; Rayner, P. J.; Norcott, P.; Green, G. G. R.; Duckett, S. B., Long-lived states to sustain SABRE hyperpolarised magnetisation. *PCCP* **2016,** *18* (36), 24905-24911.
18. Fekete, M.; Rayner, P. J.; Green, G. G. R.; Duckett, S. B., Harnessing polarisation transfer to indazole and imidazole through signal amplification by reversible exchange to improve their NMR detectability. *Magn. Reson. Chem.* **2017,** *55* (10), 944–957.

19. Truong, M. L.; Theis, T.; Coffey, A. M.; Shchepin, R. V.; Waddell, K. W.; Shi, F.; Goodson, B. M.; Warren, W. S.; Chekmenev, E. Y., 15N Hyperpolarization by Reversible Exchange Using SABRE-SHEATH. *J. Phys. Chem. C* **2015,** *119* (16), 8786-8797.
20. Pravdivtsev, A. N.; Yurkovskaya, A. V.; Vieth, H.-M.; Ivanov, K. L., RF-SABRE: A Way to Continuous Spin Hyperpolarization at High Magnetic Fields. *J. Phys. Chem. B* **2015,** *119* (43), 13619-13629.
21. Dücker, E. B.; Kuhn, L. T.; Münnemann, K.; Griesinger, C., Similarity of SABRE field dependence in chemically different substrates. *J. Magn. Reson.* **2012,** *214*, 159-165.
22. Roy, S. S.; Norcott, P.; Rayner, P. J.; Green, G. G. R.; Duckett, S. B., A Hyperpolarizable 1H Magnetic Resonance Probe for Signal Detection 15 Minutes after Spin Polarization Storage. *Angew. Chem. Int. Ed.* **2016,** *55* (50), 15642-15645.
23. Appleby, K. M.; Mewis, R. E.; Olaru, A. M.; Green, G. G. R.; Fairlamb, I. J. S.; Duckett, S. B., Investigating pyridazine and phthalazine exchange in a series of iridium complexes in order to define their role in the catalytic transfer of magnetisation from para-hydrogen. *Chem. Sci.* **2015,** *6* (7), 3981-3993.
24. Roy, S. S.; Norcott, P.; Rayner, P. J.; Green, G. G. R.; Duckett, S. B., A Simple Route to Strong Carbon-13 NMR Signals Detectable for Several Minutes. *Chem. - Eur. J.* **2017,** *23* (44), 10496-10500.
25. Olaru, A. M.; Burt, A.; Rayner, P. J.; Hart, S. J.; Whitwood, A. C.; Green, G. G. R.; Duckett, S. B., Using signal amplification by reversible exchange (SABRE) to hyperpolarise 119Sn and 29Si NMR nuclei. *Chem. Commun.* **2016,** *52* (100), 14482-14485.
26. Gloggler, S.; Muller, R.; Colell, J.; Emondts, M.; Dabrowski, M.; Blumich, B.; Appelt, S., Para-hydrogen induced polarization of amino acids, peptides and deuterium-hydrogen gas. *PCCP* **2011,** *13* (30), 13759-13764.
27. Shen, K.; Logan, A. W. J.; Colell, J. F. P.; Bae, J.; Ortiz, G. X.; Theis, T.; Warren, W. S.; Malcolmson, S. J.; Wang, Q., Diazirines as Potential Molecular Imaging Tags: Probing the Requirements for Efficient and Long-Lived SABRE-Induced Hyperpolarization. *Angew. Chem. Int. Ed.* **2017,** *56*, 12112-12116.
28. Mewis, R. E.; Green, R. A.; Cockett, M. C. R.; Cowley, M. J.; Duckett, S. B.; Green, G. G. R.; John, R. O.; Rayner, P. J.; Williamson, D. C., Strategies for the Hyperpolarization of Acetonitrile and Related Ligands by SABRE. *J. Phys. Chem. B* **2015,** *119* (4), 1416-1424.
29. Burns, M. J.; Rayner, P. J.; Green, G. G. R.; Highton, L. A. R.; Mewis, R. E.; Duckett, S. B., Improving the Hyperpolarization of 31P Nuclei by Synthetic Design. *The Journal of Physical Chemistry B* **2015,** *119* (15), 5020-5027.
30. Pravdivtsev, A. N.; Yurkovskaya, A. V.; Zimmermann, H.; Vieth, H.-M.; Ivanov, K. L., Transfer of SABRE-derived hyperpolarization to spin-1/2 heteronuclei. *RSC Adv.* **2015,** *5* (78), 63615-63623.
31. Pravdivtsev, A. N.; Yurkovskaya, A. V.; Vieth, H.-M.; Ivanov, K. L., Spin mixing at level anti-crossings in the rotating frame makes high-field SABRE feasible. *PCCP* **2014,** *16* (45), 24672-24675.
32. Holmes, A. J.; Rayner, P. J.; Cowley, M. J.; Green, G. G. R.; Whitwood, A. C.; Duckett, S. B., The reaction of an iridium PNP complex with parahydrogen facilitates polarisation transfer without chemical change. *Dalton Trans.* **2015,** *44* (3), 1077-1083.
33. Norcott, P.; Rayner, P. J.; Green, G. G. R.; Duckett, S. B., Achieving High 1H Nuclear Hyperpolarization Levels with Long Lifetimes in a Range of Tuberculosis Drug Scaffolds. *Chem. - Eur. J.* **2017,** *23* (67), 16990-16997.
34. Pavlik, J. W.; Laohhasurayotin, S., Synthesis and spectroscopic properties of isomeric trideuterio- and tetradeuterio pyridines. *J. Heterocycl. Chem.* **2007,** *44* (6), 1485-1492.
35. Pavlik, J. W.; Laohhasurayotin, S., The photochemistry of 3,4,5-trideuteriopyridine. *Tetrahedron Lett.* **2003,** *44* (44), 8109-8111.
36. Kurhanewicz, J.; Vigneron, D. B.; Brindle, K.; Chekmenev, E. Y.; Comment, A.; Cunningham, C. H.; DeBerardinis, R. J.; Green, G. G.; Leach, M. O.; Rajan, S. S.; Rizi, R. R.; Ross, B. D.; Warren, W. S.; Malloy, C. R., Analysis of Cancer Metabolism by Imaging Hyperpolarized Nuclei: Prospects for Translation to Clinical Research. *Neoplasia* **2011,** *13* (2), 81-97.

37. Eshuis, N.; Aspers, R. L. E. G.; van Weerdenburg, B. J. A.; Feiters, M. C.; Rutjes, F. P. J. T.; Wijmenga, S. S.; Tessari, M., Determination of long-range scalar 1H–1H coupling constants responsible for polarization transfer in SABRE. *J. Magn. Reson.* **2016,** *265* (Supplement C), 59-66.
38. Barskiy, D. A.; Shchepin, R. V.; Tanner, C. P. N.; Colell, J. F. P.; Goodson, B. M.; Theis, T.; Warren, W. S.; Chekmenev, E. Y., The Absence of Quadrupolar Nuclei Facilitates Efficient 13C Hyperpolarization via Reversible Exchange with Parahydrogen. *ChemPhysChem* **2017,** *18* (12), 1493-1498.

Supporting Information

Additional Supporting Information may be found online in the supporting information tab for this article.